

**THEORETICAL PREDICTIONS OF AERODYNAMIC AND DYNAMIC PHENOMENA
ON HELICOPTER ROTORS IN FORWARD FLIGHT**

Dr. C.T. Tran - Office National d'Etude et de Recherche Aéronautique

Dr. J. Renaud - SNAéronautique - Division Hélicoptères

1. INTRODUCTION

Inadequate understanding of the aerodynamics and dynamics of the helicopter rotor has contributed to limitations of improvements in rotorcraft performance. The primary factors limiting the performance of current rotary-wing aircraft are :

- Aerodynamic limitations leading to excessive power requirements, loss of lift and propulsive capability, and restrictions of manoeuvrability.
- Unsatisfactory stability characteristics and handling qualities.
- Restrictions imposed by vibration and fatigue consideration.

The field of rotor aerodynamics and dynamics, offers the most productive area of research ; a better mathematical modeling of this phenomena will improve the competitive position of helicopters in military and civilian applications (Ref. 1 to 4).

The theoretical prediction of the behaviour of a helicopter rotor is a very complex problem involving the most diversified aspects in aerodynamics and dynamics. The purpose of this paper is to describe the progress made in the theoretical methods developed by ONERA and Aérospatiale to aid engineers at the rotor design stage or during prototype development.

The rotor aerodynamics include unsteady phenomena (due to the cyclic modulation of velocities and blade angle of attack), compressibility (on the advancing blade), non-linearities (at high angle of attack on retreating blade), three-dimensional effects (due to radial flow and other phenomena at blade tip).

Further, a good knowledge of the aerodynamic field is necessary to determine the influence of the wake on the loads, and this can be done only by knowing the induced downwash distribution at the rotor disc. In the past, the rotor aerodynamic field was determined through a simplified distribution based on two-dimensional assumptions and constant induced downwash. Subsequent corrections were applied to approximately account for actual phenomena existing on the rotor.

In this paper we will use a different procedure. From a completely linear mathematical description, in both aerodynamic and dynamic aspects, the problem of determining blade loads and rotor dynamic responses is solved explicitly, in analytical form, without iteration between blade loads and responses.

The first part of this paper is devoted to aerodynamics : the linear theory of the oscillating wing (Ref. 5), which has been extended by R. Dat to take into account any arbitrary motion (Ref. 6 to 8), has been applied by J.J. Costes to the linear rotor field (Ref. 9), and then extended further to the non-linear field (Ref. 10), on the basis of results obtained in two-dimensional unsteady tests. Some simple examples of application show the importance of a good knowledge of the aerodynamic field.

The second part deals with the coupling between blade loads and responses while remaining - within the scope of this study - in the linear field (non linear aerodynamic has been introduced only in the case of rigid blades). The method developed has been applied to a flight case of an experimental helicopter, taking the rotor head motions (measured in flight), the blade dynamic characteristics (modal characteristics measured without rotation) and the aircraft characteristics into account.

2. AERODYNAMIC LINEAR ROTOR FIELD

With conventional assumptions of small disturbances, velocities and accelerations within a perfect compressible fluid are derived from potential functions satisfying the wave equation :

$$\nabla^2 \Psi - \frac{1}{a^2} \frac{\partial^2 \Psi}{\partial t^2} = 0 \quad (1)$$

This equation may be solved by a linear combination of particular solutions given by singularities placed on the airfoil. For the lifting problem, the only one dealt with in this paper, a solution with pressure discontinuity across the lifting surface, approximated by a membrane without thickness, is sought :

$$\Delta \uparrow(P, t) = -2\rho_{\infty} \Psi(P, t) \quad (2)$$

The lifting surfaces may be represented by a distribution of doublets, orientated perpendicular to the surfaces and having an amplitude equal to :

$$q(P, t) = \frac{\Delta \uparrow(P, t)}{\rho_{\infty}} \quad (3)$$

The results in an integral equation, expressing the velocity potential function at any point P of the field as a function of the lift distribution and its time history :

$$\varphi(P, t) = \int_{-\infty}^{\gamma(P)} \int_{\Sigma} K(P_0, \tau_0) \cdot q(P_0, \tau_0) d\tau_0 d\sigma \quad (4)$$

This equation is applicable to one or several lifting surfaces moving in an arbitrary manner. The kernel of the integral equation includes components of the doublets motion (position, velocity). The spatial summation is extended to the entire lifting surface, including its path space and in time, which generates a surface representing the blade rigid wake. The summation in time takes into account (through delayed potential functions) the delays in the propagation of the disturbance at finite speed.

With this approach, it is possible to include, in a mathematically accurate manner, in the linear field :

- Unsteady phenomena
- Compressibility
- Three-dimensional effects

In the case of a helicopter in steady flight, the integral equation is solved using a collocation process. The lift $\Delta p(P, t) = \rho_{\infty} q(P, t)$ is defined on a base of periodic functions having the same behaviour as the actual lift at the various blade boundaries, i.e. conforming to the Kutta condition at the trailing edge and including the singularities of the leading and side edges consistent with the kernel of the integral equation.

Due to the linearity of the integral equation, the velocity potential function (together with the velocities $V_n = \text{grad} \varphi \cdot n$) may be determined through a linear combination of elemental participations corresponding to each basic function. Thus, it is possible to determine the velocity components normal to the lifting surfaces by solving a set of linear equations. The system coefficients are influence factors, calculated from the integral equation. The numerical integrations are carried out by the Gauss Method. These coefficients form an aerodynamic matrix A . The coefficients representing the components of the lift in this representation are called pressure coefficients and constitute the vector of unknown singularities X . The flow velocities normal to lifting surfaces are the second vector of the linear system :

$$A X = V_n \quad (5)$$

Further, the lift column Γ is linearly dependant on the column X through a known transformation matrix S . The relation (5) may then be written as :

$$G \Gamma = V_n \quad (6)$$

with

$$G = A S^{-1}$$

The aerodynamic forces are then determined by compliance with the boundary conditions. These are expressed by a non-separation condition of zero normal surface velocity enforced at a number of "collocation points" distributed on the rotor disc in a mathematically optimum fashion.

At these points, column V_n of the normal flow velocities should be equal to column V_{np} of the blade normal velocities, which are calculated using the blade kinematic relations.

The solution of the system composed of the blade kinematic relations and the equation :

$$G \Gamma = V_{np} \quad (7)$$

allows the simultaneous determination of the unsteady aerodynamic loads and the blade dynamic response to these excitations.

3. NON-LINEAR AERODYNAMIC EFFECTS

When stall is present, a strong region of vorticity exists in the stalled region and its wake. The assumptions of potential flow and small disturbances remain valid in the irrotational field located outside this zone. The use of linear three-dimensional calculations when stall is present, is physically valid because, to an observer located at a point "P" sufficiently distant from the lifting surface and its wake, the thickness of the rotational zone appears negligible. Therefore the representation of the lifting surface by an area of pressure discontinuity remains valid and the integral equation linking the potential function to the lift is still valid with separated flow.

The boundary conditions are changed however. It will be assumed that for a distant observer the flow with separation is equivalent to a flow without separation around a fictitious lifting surface developing the same lift. For this equivalent flow, the normal velocities of the lifting surface are unknown since the movements of the fictitious lifting surfaces are not known a priori.

To determine these normal velocities, it is assumed that the blade segment behaves as an airfoil moving, in a two-dimensional flow, in a fluid disturbed by three-dimensional induced velocities.

The behaviour of this airfoil at high angle of attack will be deduced from wind tunnel data and the calculation of the equivalent flow without separation will be done only to determine the induced downwash, at each blade segment, due to the three-dimensional effects.

At high incidence, the linear theory is assumed to be able to furnish the actual lift providing that the profile (at incidence α) be replaced by a fictitious profile at an "effective" incidence α^* is obtained semi-empirically from experimental airfoil data. In this way, operators can be uniquely defined, with α^* expressed in terms of α and $\dot{\alpha}$ (Ref 11) or in terms of α , $\dot{\alpha}$, and $\ddot{\alpha}$ (Ref 12) :

$$\begin{aligned} \alpha^* &= g(\alpha, \dot{\alpha}) \\ &\text{or} \\ \alpha^* &= h(\alpha, \dot{\alpha}, \ddot{\alpha}) \end{aligned} \quad (8)$$

4. APPLICATION TO A ROTOR WITH HIGH ANGLES OF ATTACK

The linear equation $V_{np} = G \Gamma$ is still valid for the unseparated flow around the fictitious blades. But the velocity normal to the fictitious blades are unknown, since the motion of these blades is unknown :

$$V_{np}^* = G \Gamma^* \quad (9)$$

Since by hypothesis, each blade segment behaves as an airfoil in a two-dimensional flow, its lift is proportional to the efficient incidence α^* :

$$\Gamma^* = D \alpha^* \quad (10)$$

D is a diagonal matrix whose elements depend on fluid density and blade's velocity.

The fictitious blade normal velocities V_{np}^* may be expressed as a function of actual and effective angles of attack α and α^* by geometrical relations :

$$V_{np}^* = F(\alpha, \alpha^*) \quad (11)$$

The expressions (8) to (11) lead to a system of non linear equations which are solved by an iterative procedure. One then obtains the effective incidence α^* , and the rotor lift Γ^* including the non linear effects.

5. APPLICATION TO THE AERODYNAMIC STUDY OF A ROTOR

AEROSPATIALE applies the present theory in a simplified form where the blade is represented by a lifting line, this being admissible for the current blade shapes (Ref. 6). The accuracy of calculations is limited, of course, by the use of the lifting line theory, which is not sufficiently valid for the large variations of the downwash along the span associated with a nearby vortex (Ref. 2 and 13).

In spite of this important limitation, comparisons made with experimental results obtained on a rotor of 4.2 metres diameter, at the "S1" wind tunnel in MODANE, show that loads are estimated correctly.

In ref. 10, it has been shown that the introduction of non-linear phenomena improves the prediction of loads acting on the retreating blade (fig. 1).

Obviously, the lifting line imposes a penalty at the blade tip and in both forward and rear blade positions where some three-dimensional phenomena, not taken into account in calculations, are important.

However, such an approach, which calls on a sufficient number of major elements (non-uniform downwash, compressibility, some three-dimensional effects) allows the determination of a more accurate aerodynamic field, and, in any case, sensibly different from the one obtained using conventional methods.

Thus, figure (2) shows the distribution of the angles of attack given, on the one hand, by the present theory and, on the other hand, by a two-dimensional method with constant downwash. The structure of the two fields is rather different.

The contribution of sophisticated theories is quite obvious, as the influence of the combined effects of the variable downwash and the unsteady flow is essential to accurate determination of the aerodynamic loads. The aerodynamic diagram will be closer to reality to the extent that its mathematic expression will couple more intimately the variable downwash and the unsteady process (Ref. 14).

The variable downwash is, in fact, responsible for a greater amplitude in the upper harmonics of loads or angles of attack (fig. 3).

But, airfoil operation in the non-linear field is very sensitive to angle of attack variations.

Further, a detailed analysis of the unsteady processes is necessary as it is due to them that airfoils will react to the field of variable downwash.

At rotor design stage, often the rotor main parameters are imposed on the aerodynamicist by technological requirements. Simplified methods are then sufficient to make a first load evaluation and dimension the rotor (ref. 15), the use of a more sophisticated theory being necessary only to solve some precise problems or determine an unexplained phenomenon noted on a prototype. As an example, figure (4) shows the conventional effect of greater blade twist, with unloading of the rotor disc outer section.

But it is in the improvement of rotors, and the pushing-back of the operating range limits, that sophisticated methods may bring to the aerodynamicist useful help. In fact, experience proves that with a good airfoil adaptation to the various aerodynamic conditions met (from transonic to stalled incompressible conditions) the rotor limits may be pushed back (ref. 16). But, "before the airfoil designer can go to work, he needs to know the requirements to which he should design his new airfoil and he has to know what features are most desired in case he cannot achieve all the goals simultaneously" (ref. 2).

The improvement of the figure of merit, maximum speed, manoeuvrability or altitude flying imposes, on the aerodynamicist, some conflicting requirements relative to a better lift/drag ratio at medium " C_z " and Mach numbers, a low drag level, a higher Mach number for drag divergence at low lift value and substantial gains in C_z max. Further, to avoid excessive alternating loads, it would be necessary to have a low C_{mo} and a stable aerodynamic centre (ref. 16).

For example, figure (5) shows the pushing-back of C_z max. and drag divergence limits obtained with the SA 13109-1.58 airfoil in comparison with those of the NACA 0012 airfoil.

Thus, the compromise required for the determination of a new airfoil may be achieved through two-dimensional calculations, taking into account the predictable airfoil excursion range, determined by rotor theory.

With an iterative process, using direct and reciprocal programmes, it is possible to determine an interface between the airfoil shape and the chordwise distribution of velocities, ensuring given aerodynamic coefficients in specified conditions (on the rotor). The incompressible reciprocal methods call on conform transformations or singularities, since the introduction of compressibility causes difficulties, even in sub-critical conditions (ref. 17).

The transonic problems may be solved by hodographic methods (ref. 18 and 19), the validity of transonic two-dimensional calculations being less sure for the rotor disc outer sections. Then, the three-dimensional effects may be evaluated, in the hover flight case, using relaxation numerical methods allowing the association of a tip fairing of optimum shape to a given airfoil (ref. 20).

The theoretical evaluation of retreating blade stall poses still greater problems. Rotor experimentation brings an essential contribution to the understanding of these phenomena where numerous parameters arise and bring their own disturbances (ref. 21). The knowledge of the fundamental unsteady processes on oscillating airfoils helps greatly in this matter, in spite of experimental problems met in such tests (ref. 22).

The importance of these unsteady effects is shown, in figure (6), for two airfoils with a rotor aerodynamic field determined using the acceleration potential method.

In this case, the steady C_z max. values are experimental and the unsteady C_z max. values are determined using the method described in (ref. 11). Now the diagrams of flow over oscillating airfoils, initially developed for flat plates and wakes (ref. 23) are improved (ref. 24).

The velocity distributions thus determined are used as basis for important studies on incompressible, unsteady, laminar or turbulent boundary layer (ref. 25).

Further, the retreating blade sections located near the reverse flow region require particular processing.

They are the seat of disturbances which appear at loads getting smaller and smaller as the speed ratio increases (ref. 21). These disturbances may initiate stalling (delayed, on the other hand, in the zones distant from the reverse flow region by the oblique attack effects). These regions of low kinetic pressure are also the seat of unsteady flows which are revealed, around the critical Reynolds number, by hysteresis phenomena generated by the blade "lead-lag" motion (Ref. 26).

Finally, the airfoil unsteady characteristics will have an important dynamic impact.

The stall-flutter susceptibility of a rotor with a given airfoil may be summarily evaluated using the method described in (ref. 27).

Figure (7) shows the two- and three-dimensional aerodynamic damping coefficients characterizing these phenomena. For example, it is to be noted that excessive spanwise blade slenderness or a great susceptibility of the airfoil to the leading edge surface finish (and to sudden transitions) (ref. 28) may be detrimental.

6. SUMMARY OF THE DYNAMIC PROBLEM

The dynamic characteristics of the complete structure may be conveniently described either by branch modes which characterize the blades and fuselage separately (Ref. 29), or by a transfer function at the rotor hub.

The theory has been applied to a three bladed semi-articulated rotor in which the orientation of the axis of rotation is fixed with respect to the free stream velocity at infinity. The angular velocity of the rotor is constant and the oscillatory movements of the rotor hub are included. In the present report, however, the rotor hub movements have been measured during the flight tests and will therefore be considered as known excitation functions. The analysis is restricted to steady forward flight conditions where both the aerodynamic loading and the blade vibratory responses are periodic functions of time.

The blades have linear twist and are articulated both in flap and lead-lag. The blade lead-lag motion is restrained by visco-elastic dampers that provide both stiffness and damping. The flapping hinge is located radially inboard of the feathering bearing. The lead-lag hinge is located radially outboard of the feathering bearing and thus will rotate as the blades change pitch (NAT rotor head, GAZELLE Production).

The vibratory movements of the blades are represented by a set of fully coupled (flap, lead-lag and torsion) normal modes of the non rotating cantilevered blade, together with two articulated rigid body modes (flap and lead-lag). These rigid body modes are non orthogonal to the cantilevered set. Effects of the centrifugal forces are introduced separately.

Application of the Coleman transformation to the system of Lagrange equations leads to a set of linear ordinary differential equations with constant coefficients in terms of the rotor generalized coordinates.

The coupling of the structural dynamics with the linear aerodynamic forces is accomplished through the Aerodynamic influence matrix A whose elements have been computed, based on the hypothesis of small perturbations, independent of the blades vibratory movements. The Aerodynamic influence matrix relates the aerodynamic pressure coefficients to the blades normal velocities which in turn, through a kinematic relation, are related to the rotor generalized coordinates. The problem is then solved by a Collocation Method leading to simultaneous solutions for the aerodynamic loading and the blades vibratory response.

7. PROBLEM FORMULATION

Lagrange equations in terms of the rotor generalised coordinates are employed to describe the dynamics of the structure. The system is first defined in terms of a set of generalized coordinates consisting of the cantilevered modes of the non-rotating blade and two articulated rigid body modes. The rotor hub motion is also included.

The kinetic energy of the rotor is then expressed in terms of the blade's generalized mass matrix M , a matrix Φ arising from the centrifugal forces and terms that originate from the gyroscopic coupling of the blades and rotor hub motions.

The potential energy of the rotor is expressed by a diagonal stiffness matrix K which includes the stiffness contribution of the visco-elastic damper. The dissipation function is expressed by a generalized damping matrix B representing both the blades structural damping and the viscous damping due to the visco-elastic damper.

For a three-bladed rotor, for example, the Coleman transformation is :

$$\Delta \kappa = \kappa_1 + \kappa_2 \cos \psi \kappa + \kappa_3 \sin \psi \kappa \quad \text{where} \quad \psi \kappa = \Omega t + 2(\kappa - 1) \pi / 3$$

and $y = \begin{pmatrix} \kappa_1 \\ \kappa_2 \\ \kappa_3 \end{pmatrix}$ are the rotor generalized coordinates.

This transformation may be applied to the Lagrange equations, leading to a set of linear ordinary differential equations with constant coefficients :

$$m \ddot{y} + B \dot{y} + Ky = Q + \mathcal{Q} \sum_{n=1}^2 D_n e^{jn\Omega t} + Q_a$$

where :

Q : is a constant column vector depending on the cyclic pitch command, the drag arising from the air viscosity, and the blade weight.

D_n : is a complex column vector accounting for the excitation of the rotor due to the known rotor hub movement and air viscosity.

Q_a : is the unknown generalized aerodynamic forces column.

As seen in the description of the linear aerodynamic problem, the aerodynamic forces were written in terms of periodic functions with the unknown pressure coefficients X.

Assuming that the lift forces are normal to the blade surfaces, the virtual work is linearly dependant on Y, and Q_a is shown to be :

$$Q_a = G_0 X + \sum_{n=1}^2 G_n X e^{3jn\omega t}$$

where G_0 and G_n are known matrix depending on the mode shapes.

It is observed that the generalized forces (in the right hand side rotor coordinates) are restricted to functions of constant, 3rd and 6th harmonic quantities for a three-bladed rotor.

Combination with the aerodynamic equation and the kinematic relation leads to the simultaneous solutions for the columns X and Y.

8. APPLICATION TO WIND TUNNEL AND FLIGHT TEST

The modal method combined with the linear aerodynamics as given by the acceleration potential theory has been applied to a rotor model tested in the RAE tunnel (case 52) and to a case of flight test results of a research helicopter (SA 349Z GAZELLE). Comparisons are made between the calculated and the measured blade bending moments.

The RAE model is a three bladed rotor of 3 m diameter. The blades, with flap and lead lag flexures near the root are cantilevered to the hub. The motion of the hub has been neglected in the analysis and only cantilevered modes are required to describe the blade motions. The test advance ratio is .19 and the collective pitch is adjusted to provide a rotor lift of 174 lbs. The comparisons (fig. 8) show that good agreement for both the flat wise and edgewise bending moments is obtained.

In the comparison with the results of a flight test, NAT rotor head (described previously) measured oscillatory movements have been included in the analysis. The flight test advance ratio is .33. Fig (9) shows the good correlation on the blade flatwise bending moments.

The slight influence of the rotor head motion on the blade flatwise moments is also presented. The predictions of the blade lead-lag bending moments require that additionnal second order terms be incorporated in the analysis. These terms include the induced drag and Coriolis forces. This work is being carried out presently.

9. CONCLUSION

The representation of a lifting surface by a set of acceleration "doublets" allows the expression, in the linear field, of the three-dimensional, compressible and unsteady phenomena generated in a rotor.

Even when the expression is reduced to a lifting line, the prediction of rotor loads is correct and may be improved by taking the retreating blade non-linear phenomena into consideration. The aerodynamic field accuracy obtained allows a better definition of the airfoil operating envelope and leads to a judicious application of two-dimensional methods of airfoil calculations.

This aerodynamic diagram may be coupled to a modal representation of blades to solve, in the linear field, the rotor dynamic problems, in an analytical form without iteration between the blade loads and responses.

The research effort must be continued to arrive at a better representation of three-dimensional effects in aerodynamics, and non-linear phenomena in dynamics.

REFERENCES

- (1) J.P. JONES
Rotors aerodynamics - retrospect and prospect
(AGARD Advisory report 13, aspect of V/STOL aircraft development, Sept. 1967)
- (2) P.F. YAGGY I.C. STATLER
Progress in rotor-blade aerodynamics
(AGARD Conference Proceedings N° 121, advanced rotorcraft, Sept. 1971)
- (3) P.F. YAGGY
The role of aerodynamics and dynamics in military and civilian applications of rotary wing aircraft
(AGARD lecture series N° 63)
- (4) G. PETIT
Grandes tendances actuelles de l'hélicoptère
(L'Aéronautique et l'Astronautique N° 48, 1974-5)
- (5) H.G. KUSSNER
General Airfoil theory
(NACA TM 979, 1941)
- (6) R. DAT
Représentation d'une ligne portante animée d'un mouvement arbitraire par une ligne de doublets d'accélération.
(Recherche Aérospatiale N° 133 - 1969)
- (7) R. DAT
Unsteady aerodynamics of wings and blades
(Symposium IUTAM/IAHR : flow-induced structural vibrations - Karlsruhe - Août 1972)
- (8) R. DAT
La théorie de la surface portante appliquée à l'aile fixe et à l'hélice.
(Recherche Aérospatiale N° 1973 - 4)
- (9) J.J. COSTES
Calcul des forces aérodynamiques instationnaires sur les pales d'un rotor d'hélicoptère.
(AGARD Report N° 595).

- (10) J.J. COSTES
Introduction du décollement instationnaire dans la théorie du potentiel d'accélération, application à l'hélicoptère.
(Recherche Aérospatiale N° 1975 - 3)
- (11) R.E. GORMONT
A mathematical model of unsteady aerodynamics and radial flow for application to helicopter rotors
(USAAMRDL Technical Report 72 - 67)
- (12) F.O. CARTA G.L. COMMERFORD
R.G. CARLSON R.H. BLACKWELL
Investigation of airfoil dynamic stall and its influence on helicopter control loads.
(USAAMRDL Technical Report 72 - 51)
- (13) JOHNSON WAYNE
Application of a lifting-surface theory to the calculation of helicopter airloads
(Reprint N° 510, 27th Annual V/STOL Forum AHS May 1971)
- (14) A.J. LANDGREBE M.C. CHENEY
Rotors wakes - Key to performance prediction
(AGARD Conference Proceedings N° 111 - Marseille - Sept. 1972)
- (15) J. GALLOT
Calcul des charges sur rotor d'hélicoptère
(AGARD Conference Proceedings N° 122 - Milan - March 1973)
- (16) P. FABRE
Problèmes de trainées des appareils à voilures tournantes.
(AGARD Lecture Series N° 63 - Brussels - April 1973)
- (17) G. REICHERT Dr. S.N. WAGNER
Some aspects of the design of rotor-airfoil shapes
(AGARD Conference Pre-print N° 111 - Marseille - Sept. 1972)
- (18) G. NIEUWLAND
Transonic potential flow around a family of quasi-elliptical aerofoil sections.
(NLR Amsterdam, Report TR.T. 172, 1.967)

- (19) P. GARABEDIAN D. KORN
Numerical design of transonic airfoils
(Numerical solution of partial differential equations, II, Academic Press, 1971)
- (20) W.F. BALLHAUS F.X. CARADONNA
The effect of planform shape on the transonic flow past rotor tips
(AGARD Conference Pre-print N° 111 - Marseille - Sept. 1972)
- (21) M. LECARME
Comportement d'un rotor au delà du domaine de vol usuel à la grande soufflerie de Modane
(AGARD Conference Pre-print N° 111 - Marseille - Sept. 1972)
- (22) J. COULOMB
Mesures instationnaires sur le profil NACA 0012 en oscillations harmoniques de tangage.
(C.E.A.T. P.V. d'essais)
- (23) T. THEODORSEN
General theory of aerodynamic instability and the mechanism of flutter
(NACA Report 496, 1935)
- (24) W.J. Mc CROSKEY
Inviscid flow field on oscillating airfoil
(J.A.I.A.A. Vol. 11 N° 8 - Aug. 1973)
- (25) W.J. Mc CROSKEY J.J. PHILIPPE
Unsteady viscous flow on oscillating airfoils
(AIAA Journal - Vol. 13 N° 1 - Janv. 1975)
- (26) J. VALENSI, J.M. REBONT, J. RENAUD, G. VINGUT
Efforts aérodynamiques sur un profil d'aile animé d'un mouvement harmonique de tamis.
(AGARD Conference Pre-print N° 111 - Marseille - Sept. 1972)
- (27) N.D. HAM
An experimental investigation of stall flutter
(J. A.H.S. - Janv. 1962)

- (28) H.H. PEARCEY P.G. WILBY
M.J. RILEY P. BROTHERHOOD
The derivation and verification of a new rotor profile on the basis of flow phenomena ; aerofoil
research and flight tests.
(R.A.E. Technical Memorandum Aero 1440)
- (29) R. DAT
Aeroelasticity of rotary-wing aircraft
(AGARD Lecture Series N° 63 on helicopter aerodynamics and dynamics)

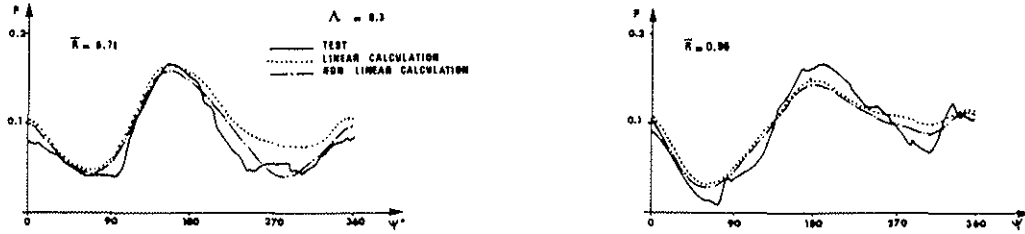


Fig. 1 - Non-dimensional lift versus azimuth -
Modane wind-tunnel rotor model
(Three-bladed rotor, $CT/\sigma = 0,092$)

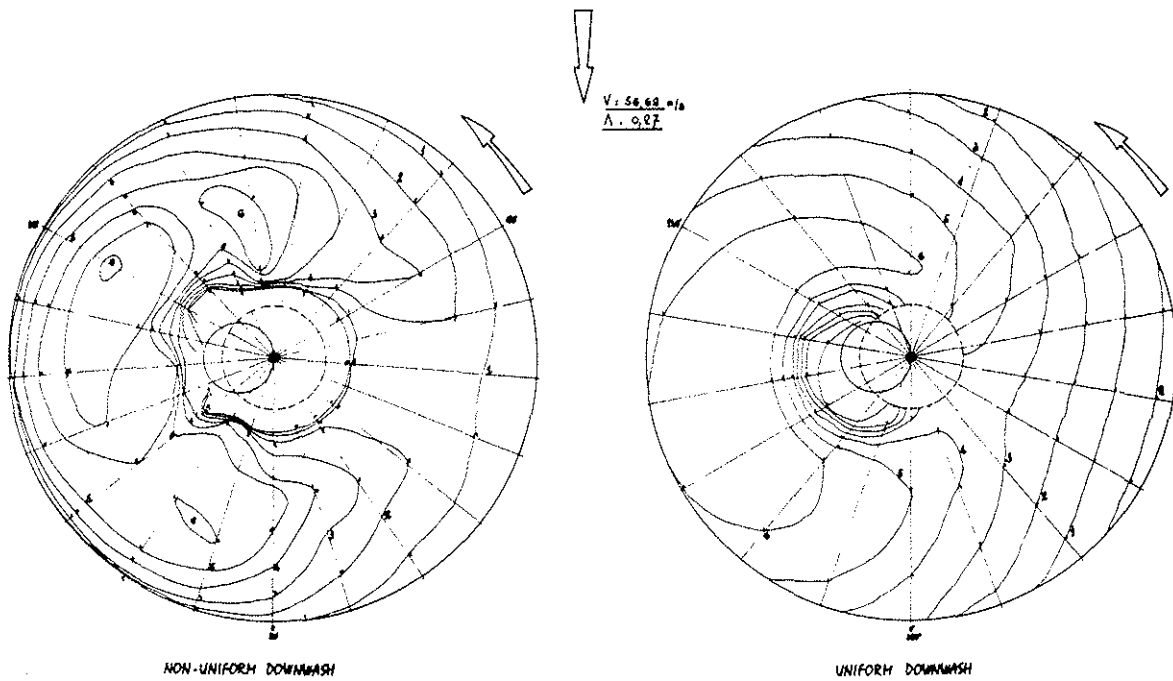


Fig. 2 - Angle of attack distribution
(Four-bladed rotor, $CT/\sigma = 0,063$, $Z = 3\ 280$ ft)

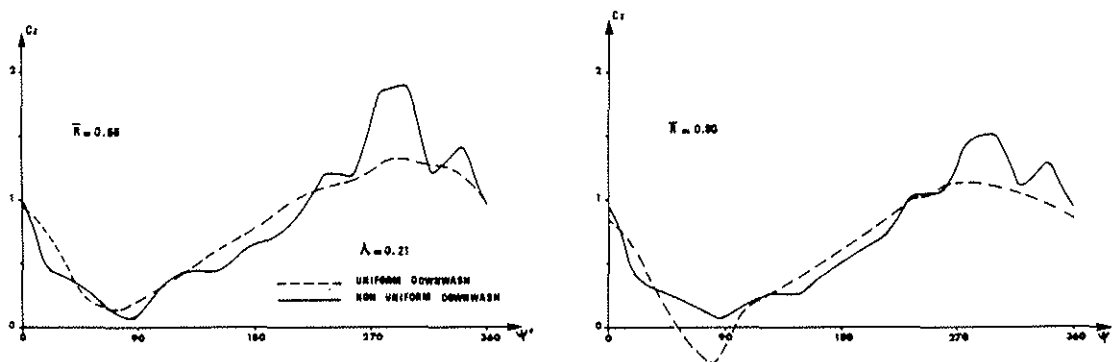


Fig. 3 - Influence of the downwash model on the lift distribution
(Four-bladed rotor, $CT/\sigma = 0,077$)

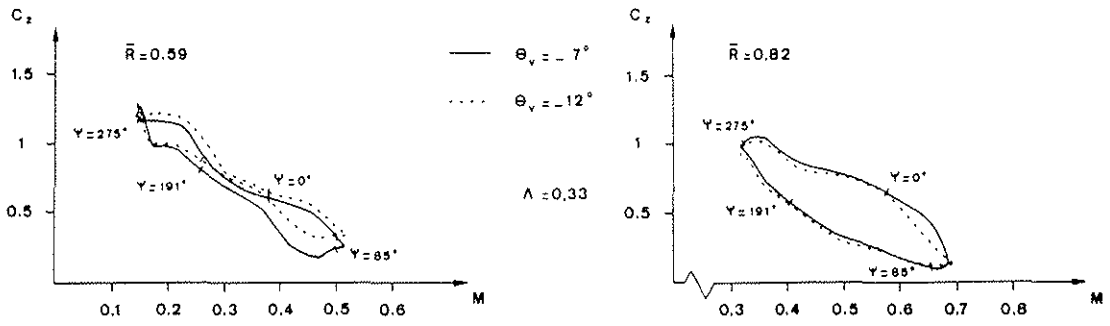


Fig. 4 - Blade twist influence on the airfoil operating range
(Three-bladed rotor, $CT/\sigma = 0,067$, $Z = 1\ 650$ ft)

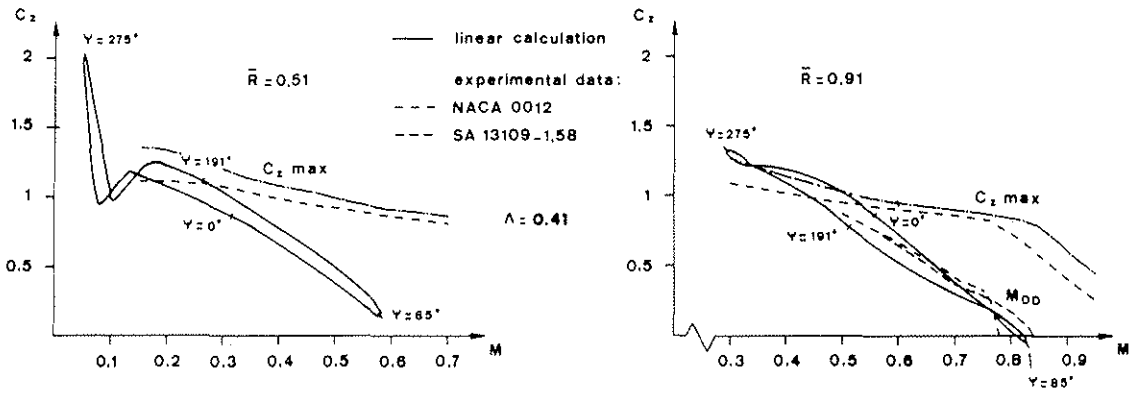


Fig. 5 - Influence of airfoil type on operating range limitations by steady stall and drag divergence
(Three-bladed rotor, $CT/\sigma = 0,073$, $Z = 3\ 280$ ft)

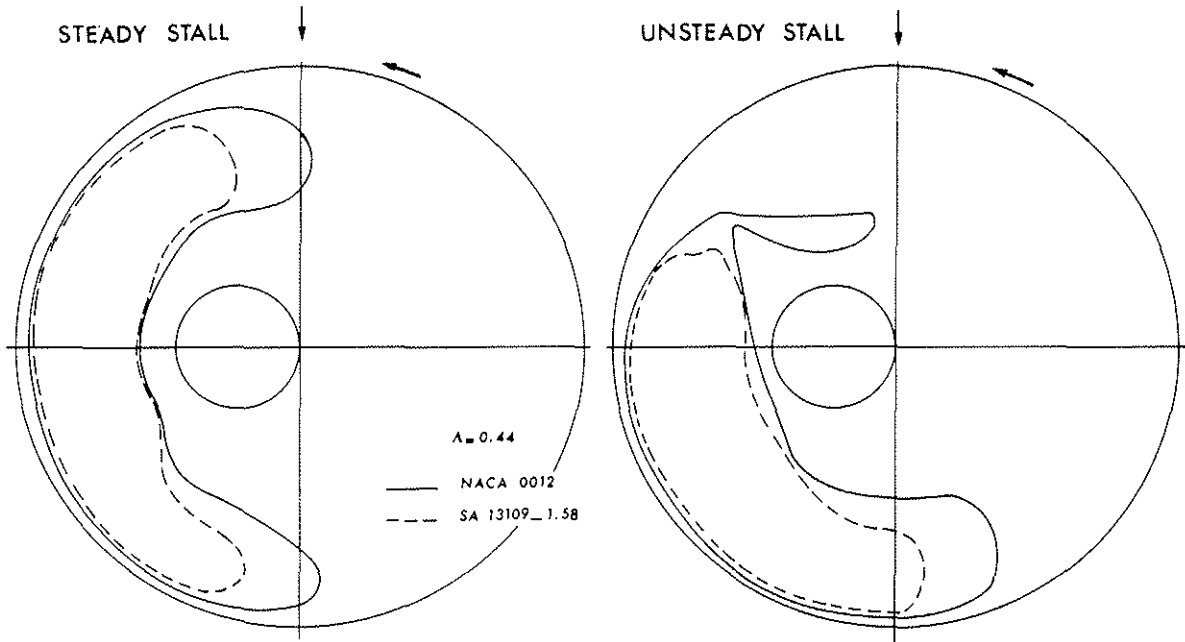


Fig. 6 - Influence of unsteadiness on the lift stall area
(Three-bladed rotor, $CT/\sigma = 0,073$, $Z = 3\ 280$ ft)

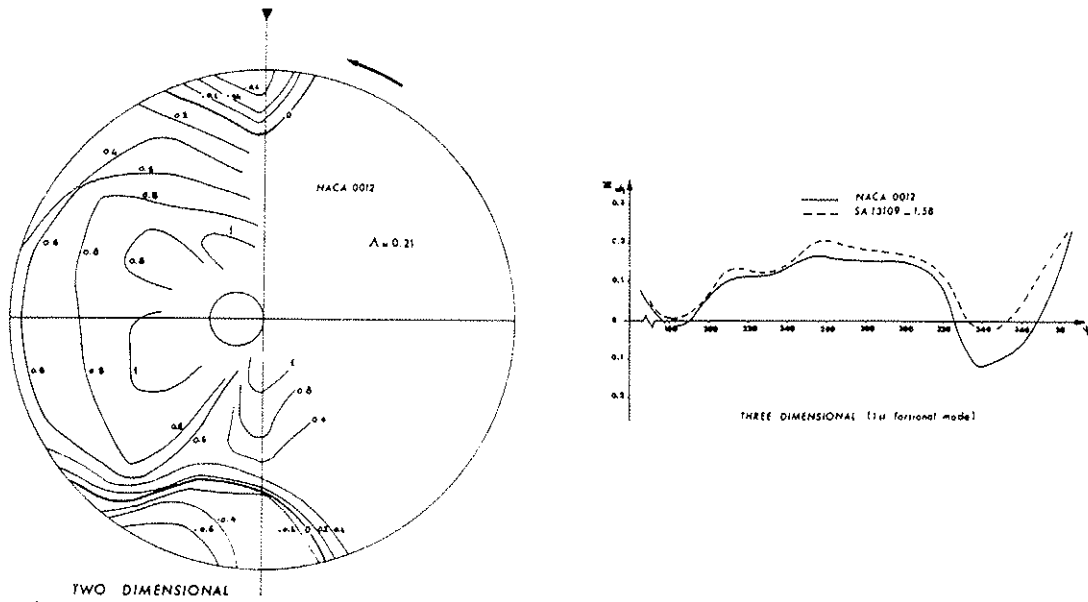


Fig. 7 - Reduced aerodynamic damping
 (Four-bladed rotor, $CT/\sigma = 0,077$)
 $\theta_v = -8,9^\circ$, $Z = 3\ 280$ ft)

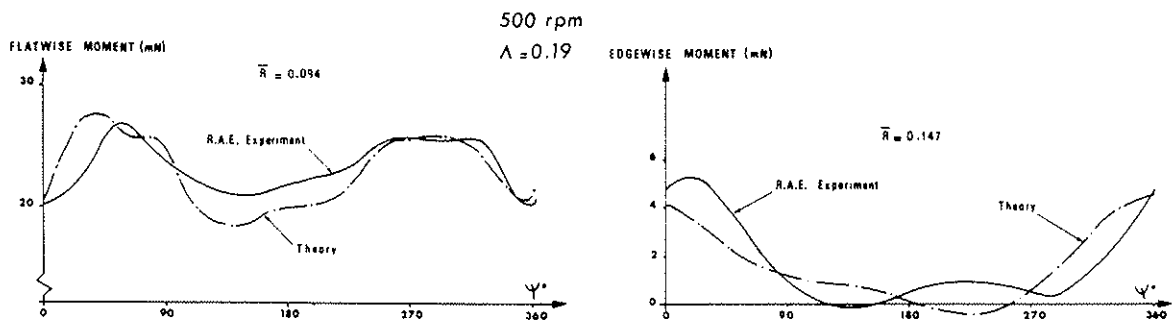


Fig. 8 - Bending moments history on R.A.E. Model rotor

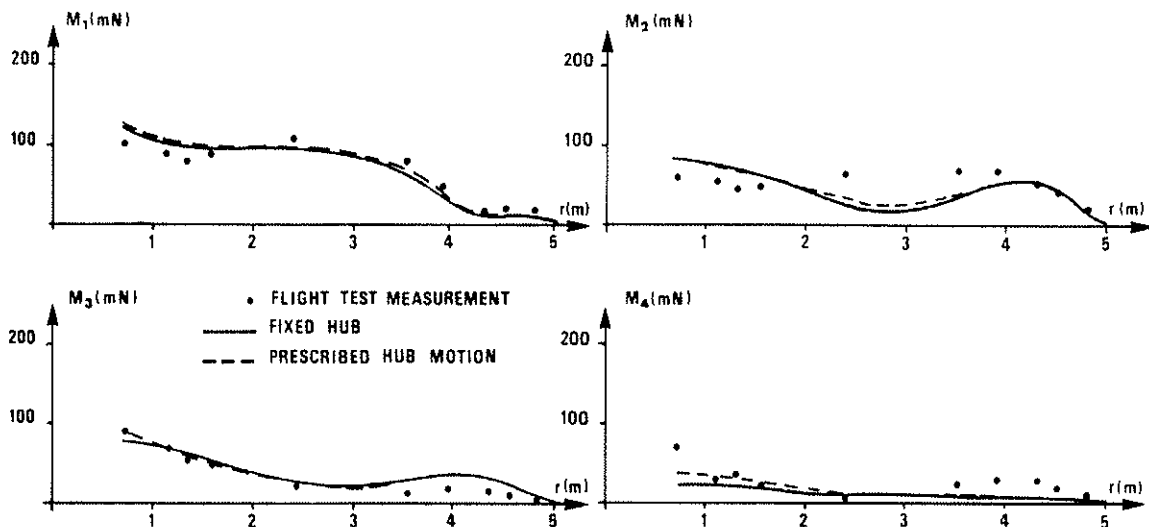


Fig. 9 - SA 349 Flatwise bending moment amplitudes
 Harmonic analysis ($\Lambda = 0,33$, $CT/\sigma = 0,067$)